Scientific Research Publishing

Energy and Power Engineering, 2017, 9, 53-62
http://www.scirp.org/journal/epe
ISSN Online: 1947-3818
ISSN Print: 1949-243X

Analysis of Non-Sinusoidal Steady Electric Field of ±500 kV Converter Transformer

Gang Liu[1*], Cheng Chi[1], Yanjiao Jin[1], Yongqiang Ma[1], Lipeng Sun[1], Lin Li[2], Youliang Sun[3]

[1]Hebei Provincial Key Laboratory of Power Transmission Equipment Security Defense, North China Electric Power University, Baoding, China
[2]State Key Laboratory of Alternate Electrical Power System with Renewable Energy Sources, North China Electric Power University, Beijing, China
[3]Shandong Power Equipment Co., Ltd., Jinan, China
Email: *liugang_em@163.com

How to cite this paper: Liu, G., Chi, C., Jin, Y.J., Ma, Y.Q., Sun, L.P., Li, L. and Sun, Y.L. (2017) Analysis of Non-Sinusoidal Steady Electric Field of ±500 kV Converter Transformer. *Energy and Power Engineering*, **9**, 53-62.
https://doi.org/10.4236/epe.2017.94B007

Received: January 13, 2017
Accepted: March 30, 2017
Published: April 6, 2017

Abstract

The line side winding is under the fundamental frequency AC voltage, while the valve side winding contains not only fundamental AC voltage component, but also the DC voltage component, fundamental AC voltage component, and higher harmonic voltage components when the converter transformer is at its normal operating condition, and the electric field of converter transformer is a non-sinusoidal steady one. To analyze the non-sinusoidal steady electric field containing the DC component, fundamental AC and higher harmonic components, the voltage spectrum of the valve winding in a ±500 kV converter transformer is firstly analyzed, and the non-sinusoidal periodic steady electric field is obtained by the fast discrete Fourier transform. Different resistivity of the oil and oil-immersed paper is adopted to simulate the aging of oil paper insulation at operation, and get the non-sinusoidal steady electric field.

Keywords

Converter Transformer, AC-DC Hybrid, Non-Sinusoidal, Periodic, Electric Field

1. Introduction

As one of the important equipment in HVDC transmission project, the safe operation of converter transformer is directly related to the stability of the system [1]. Though the converter transformer is different from AC transformer in structure and performance, the oil-paper insulation is still the main insulation of high voltage bushing. When converter transformer in normal operation, the line

side winding is under AC voltage, and the valve side winding is under AC-DC hybrid voltage, meanwhile they also withstand higher harmonic voltage caused by converter valve, thus oil paper in winding is subjected to DC, AC and higher harmonic voltage. The electric field distribution is decided by the resistivity and permittivity of oil and oil immersed paper, while the resistivity ratio of oil and oil immersed paper is generally between 1:10 - 1:300. However when the insulation aging, the ratio can be up to 1:1 or 1:1000. So it's necessary to analyze AC-DC hybrid electric field affected by the insulation aging [2].

The polarity reversal electric field of converter transformer has been analyzed in some paper [3]-[15]. There is some analysis of the periodic non-sinusoidal steady hybrid electric field, yet the electric field is always assumed to be under the fundamental frequency AC and DC voltage [16]. Actually the valve side winding of converter transformer also withstands high harmonic electric field [17].

For simplicity, the anisotropy of the oil press-paper and the nonlinearity of the insulation between conductivity and electric field strength are not taken into consideration. A two-dimensional periodic non-sinusoidal steady hybrid electric field of a ±500 kV converter transformer with different resistivity ratio is calculated and compared.

2. FEM Equation of Frequency Domain

The periodic non sinusoidal steady hybrid electric field in converter transformer belongs to quasi-static field. In this condition, the initial boundary problem based on scalar potential φ is as follows [18]:

$$\begin{cases} \nabla\cdot\left(\varepsilon\dfrac{\partial}{\partial t}+\gamma\right)\nabla\varphi=0,\varphi\in\Omega \\ \varphi|_{\Gamma_1}=u(t) \\ \dfrac{\partial\varphi}{\partial n}|_{\Gamma_2}=\psi(t) \\ \varphi|_{t=0}=\varphi(0) \end{cases} \qquad \Gamma_1+\Gamma_2=\partial\Omega \tag{1}$$

Ω is for computed area; Γ_1 and Γ_2 are the first kind of boundary condition and the second kind of boundary condition respectively. The area Ω is triangularly meshed and the unit potential is linear interpolated in each area. The semi-discrete differential equation with nodal potential by Galerkin finite element method:

$$\boldsymbol{K}_\varepsilon\frac{\partial\boldsymbol{\varphi}}{\partial t}+\boldsymbol{K}_\gamma\boldsymbol{\varphi}=\boldsymbol{F} \tag{2}$$

$\boldsymbol{K}_\varepsilon$, $\boldsymbol{K}_\gamma$—finite element stiffness matrix, $\boldsymbol{\varphi}$—potential column vector, $\boldsymbol{F}$—second kinds of boundary conditions.

For the $\boldsymbol{K}_\gamma$ is constant without considering electric field strength, temperature or other factors, so it's easy to obtain non sinusoidal periodic steady electric field by frequency finite element [19]. Equation (2) can be changed into the following form, by using the fast Fourier transform [20].

$$j2\pi k\Delta_f \boldsymbol{K}_\varepsilon \left[\frac{1}{N}\sum_{k=0}^{N-1}\boldsymbol{\Phi}_f\left(k\Delta_f\right)e^{j\frac{2\pi}{N}k}\right]+\boldsymbol{K}_\gamma\left[\frac{1}{N}\sum_{k=0}^{N-1}\boldsymbol{\Phi}_f\left(k\Delta_f\right)e^{j\frac{2\pi}{N}k}\right]=0 \quad (3)$$

Then we can get:

$$\left[\boldsymbol{K}_\gamma + j2\pi k\Delta_f \boldsymbol{K}_\varepsilon\right]\boldsymbol{\Phi}_f\left(k\Delta_f\right)=0 \quad (4)$$

The first kind of boundary conditions is also converted by FFT, and each frequency point $k(k = 0,1, \ldots, N/2)$ would be imposed boundary conditions according to Equations (4). After it is obtained, non-sinusoidal periodic steady results in the original time domain can be calculated by Fast Fourier inverse transform. It is worthy that: according to Fourier transform, Equations (4) only need to be calculated for $k = 0,1, \ldots, N/2$, then the value of $\varphi(n\Delta_t)$ $(n = 0,1, \ldots, N)$ can be obtained based on the fact that $\varphi(n\Delta_t)$ is real number and has the characteristics of periodic function.

3. Period Non Sinusoidal Steady Voltage ±500 kV of Converter Transformer

According to the actual parameters of Three Gorges-Changzhou HVDC project, the model has been established with a AC system with converter transformer, converter valve, AC/DC filter, flat wave reactor, transmission line, control system by PSCAD/EMTDC. The period of the steady voltages on valve side winding are shown in the left of **Figure 1** and **Figure 2**, and the spectrum analysis of their

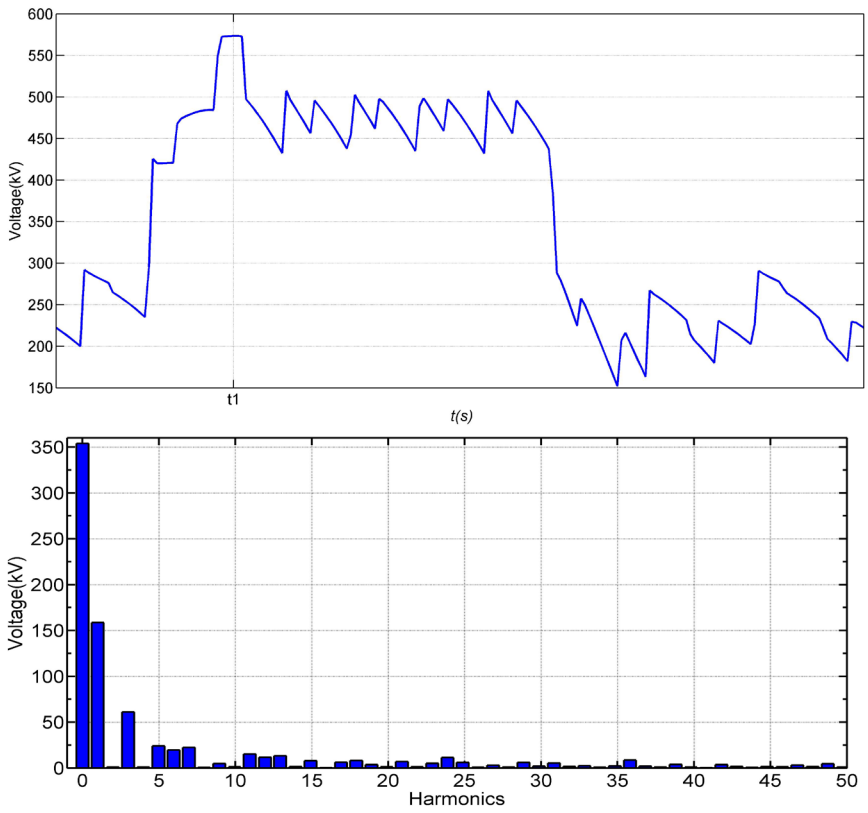

Figure 1. Periodic voltage curves and discrete frequency spectrum of the Y_0-Δ converter transformer.

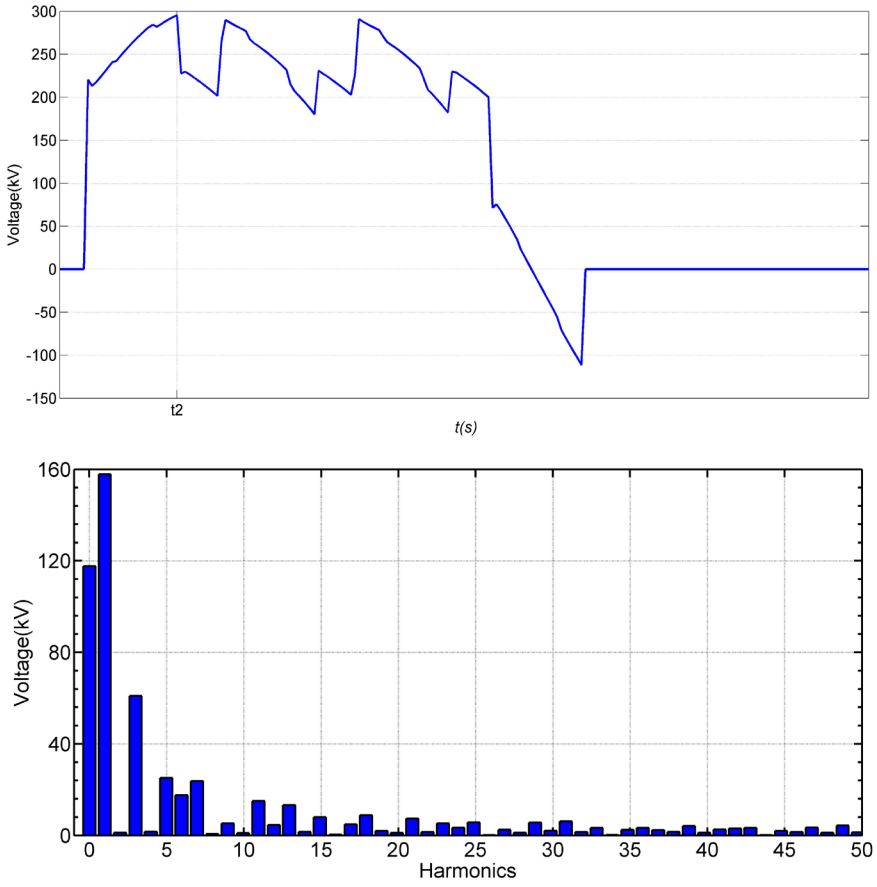

Figure 2. Periodic voltage curves and discrete frequency spectrum of the Y_0-Y converter transformer.

voltage are illustrated in the right of **Figure1** and **Figure 2**. Two time instant t_1 and t_2 are shown in the left of **Figure 1** and **Figure 2**, and they are the local maximum over one period of Y_0-Δ and Y_0-Y connected valve side winding.

From frequency spectrum of the **Figure 1** and **Figure 2**, the valve side winding includes not only DC voltage and the fundamental frequency AC voltage, but also a lot of high harmonics whose amplitude is large (for example the amplitude of the 3rd harmonic is 60 kV.) If the hybrid electric field only includes DC and fundamental frequency AC components, the results will be different from the actual one.

In this paper, the steady AC-DC hybrid electric field is obtained by the frequency domain FEM, which is to consider the DC, fundamental and high harmonic voltage components, and the inverse fast Fourier transform method.

4. Model of Converter Transformer

The two-dimensional simplified model of a ±500 kV converter transformer is triangularly meshed. There are 153,692 elements and 79,929 nodes. 4 sets of resistivity are given in **Table 1**, while the relative permittivity of transformer oil, oil immersed pressed-paper and insulation paper are 2.2, 4.5 and 3.5 [2], due to their small changing ranges.

Table 1. Values of resistivity.

Values of Resistivity in Three Materials (Unit: Ω·m)	Properties of Different Insulating Materials		
	Oil	Insulation Paper	Oil immersed pressed paper
A1	10^{12}	10^{12}	10^{12}
A2	10^{12}	5×10^{12}	10^{13}
A3	10^{12}	5×10^{13}	10^{14}
A4	10^{12}	5×10^{14}	10^{15}

5. Analysis of Compound Electric-Field of ±500 kV Converter Transformer

The hybrid electric-field potentials of the ±500 kV converter transformer at different resistivity ratio are given in **Figure 3** and **Figure 4**. **Figure 3** shows the potential contour at time t_1 as **Figure 1(a)** in Y_0-Δ connected converter transformer; **Figure 4** shows the potential contour at t_2 as **Figure 2(a)** in Y_0-Y connected converter transformer.

More equi-potential lines focus on oil immersed paper when the oil resistivity ratio changing from 1:1 to 1:1000, because the electric field is proportional to the oil resistivity when the valve side winding contains DC voltage.

The maximum electric field with time of transformer oil, oil immersed paper and insulation layer is given in **Figure 5** and **Figure 6**; the maximum electric field of various media is given in **Table 2** and **Table 3** in one period.

The maximum electric field curve with time from various media is comprised in shown as **Figure 5** and **Figure 6**: The maximum electric field strength curve is not the result of DC and fundamental AC, but also caused by high harmonic voltage on valve side winding and the fundamental frequency AC on network side winding.

The maximum electric field curves with time vary in different media when the resistivity ratios of oil paper are equal, because the DC component in Y_0-Δ connected converter transformer(about 350 kV) is much larger than that of Y_0-Y connected one (about 120 kV). The curve of electric field with time is relatively smooth in some intervals, but at some instants the curve is similar to the voltage curve of the valve side winding. The maximum point on the smoother curve is corresponding to the line side winding, and some is corresponding to the valve side winding.

When the oil resistivity changes a lot, the maximum electric field strength of oil, oil paper and insulation layer alters greatly (as **Figure 5**, **Figure 6**, **Table 2**, **Table 3**). e.g. the maximum electric field strength of oil, insulating layer and oil paper is respectively 6.16 kV/mm, 31.06 kV/mm and 45.38 kV/mm while the resistivity rate is 1:500:1000; the maximum is respectively 9.07 kV/mm, 11.23 kV/mm and 5.19 kV/mm while the resistivity rate is 1:1:1. The change of the maximum electrical field is similar to that of the oil resistivity. In the initial operation, the resistivity of oil, insulation layer and paper is higher (e.g. the resistivity ratio of the oil, insulation layer and pressboard 1:500:1000), after running

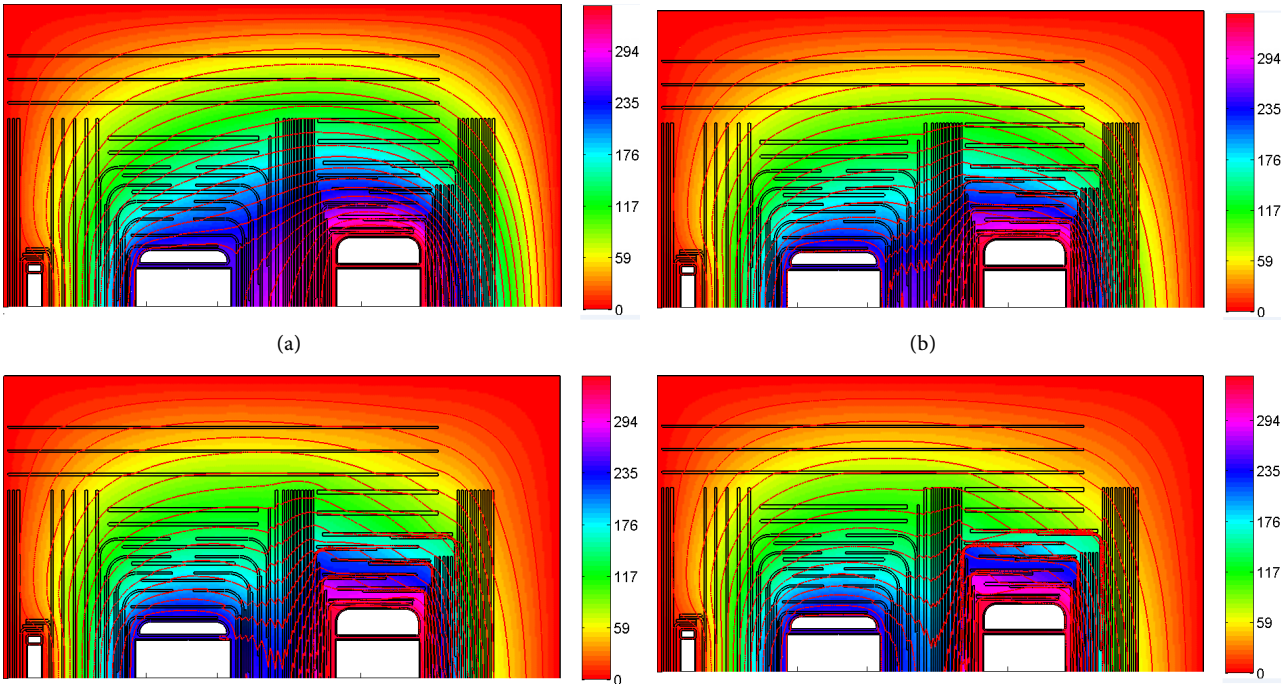

Figure 3. The potential distribution of the Y_0-Δ connected converter transformer at different condition. (a) values A1. (b) values A2. (c) values A3. (d) values A4.

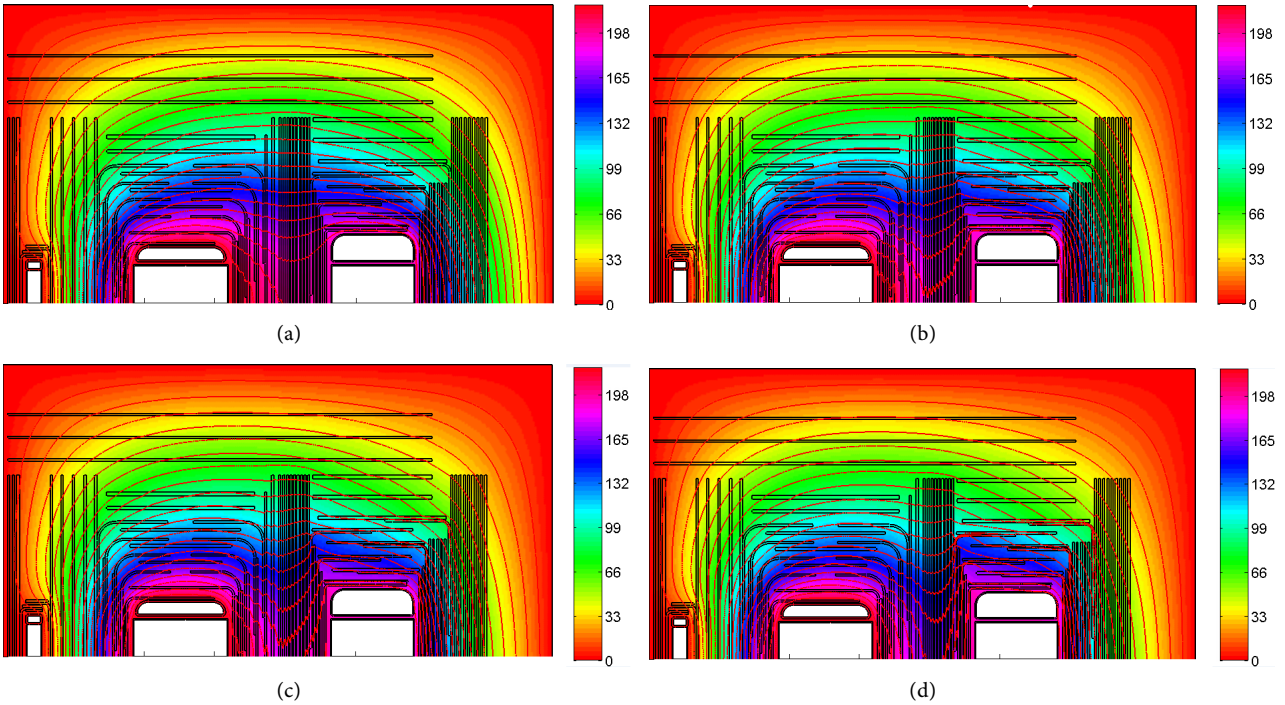

Figure 4. The potential distribution of the Y_0-Y connected converter transformer at different condition. (a) values A1. (b) values A2. (c) values A3. (d) values A4.

for some time, the resistivity of aging media will reduced (e.g. the resistivity ratio of the oil, insulation layer and pressboard 1:1:1 in extreme cases). It is beneficial for the insulation of oil immersed paper when the maximum electric field

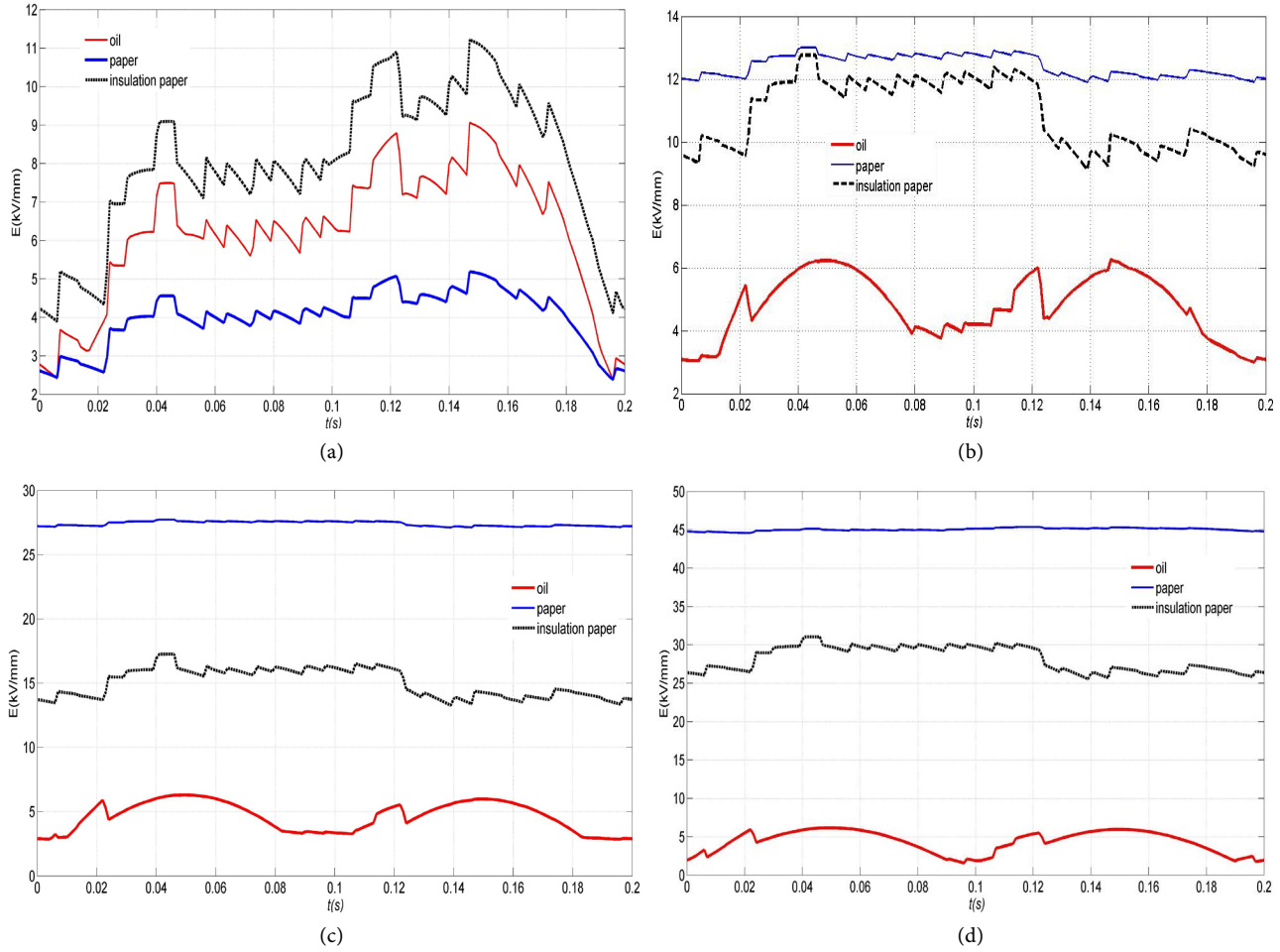

Figure 5. Electric field curves in different materials in a period of the Y_0-Δ connected converter transformer. (a) values A1. (b) values A2. (c) values A3. (d) values A4.

strength of oil and insulation layer decreases while the voltages of network and valve side winding are invariable. Actually it's harmful for the oil insulation when the maximum electric field of oil increases from 6.16 kV/mm to 9.07 kV/mm. Therefore the effects of the resistivity aging on electric field should be taken consider into the converter transformer design.

6. Conclusion

The finite element method in frequency domain and the fast inverse Fourier transform method are used to obtain the steady AC-DC hybrid electric field in this paper. The resistivity ratio of oil and oil immersed paper have been changed, meanwhile the relative permittivity kept unchanged, to simulate the aging process of oil immersed paper after long time operation. More equip-potential lines tend to locate at pressed paper with increasing ratio. However, the curve of the maximum electric field intensity with time is not the same within different media even the resistivity ratios of paper are unchanged, because the DC component in Y_0-Δ is not the same as in Y_0-Y connected one. Meanwhile the maximum electric field of insulation paper increases obviously and the maximum

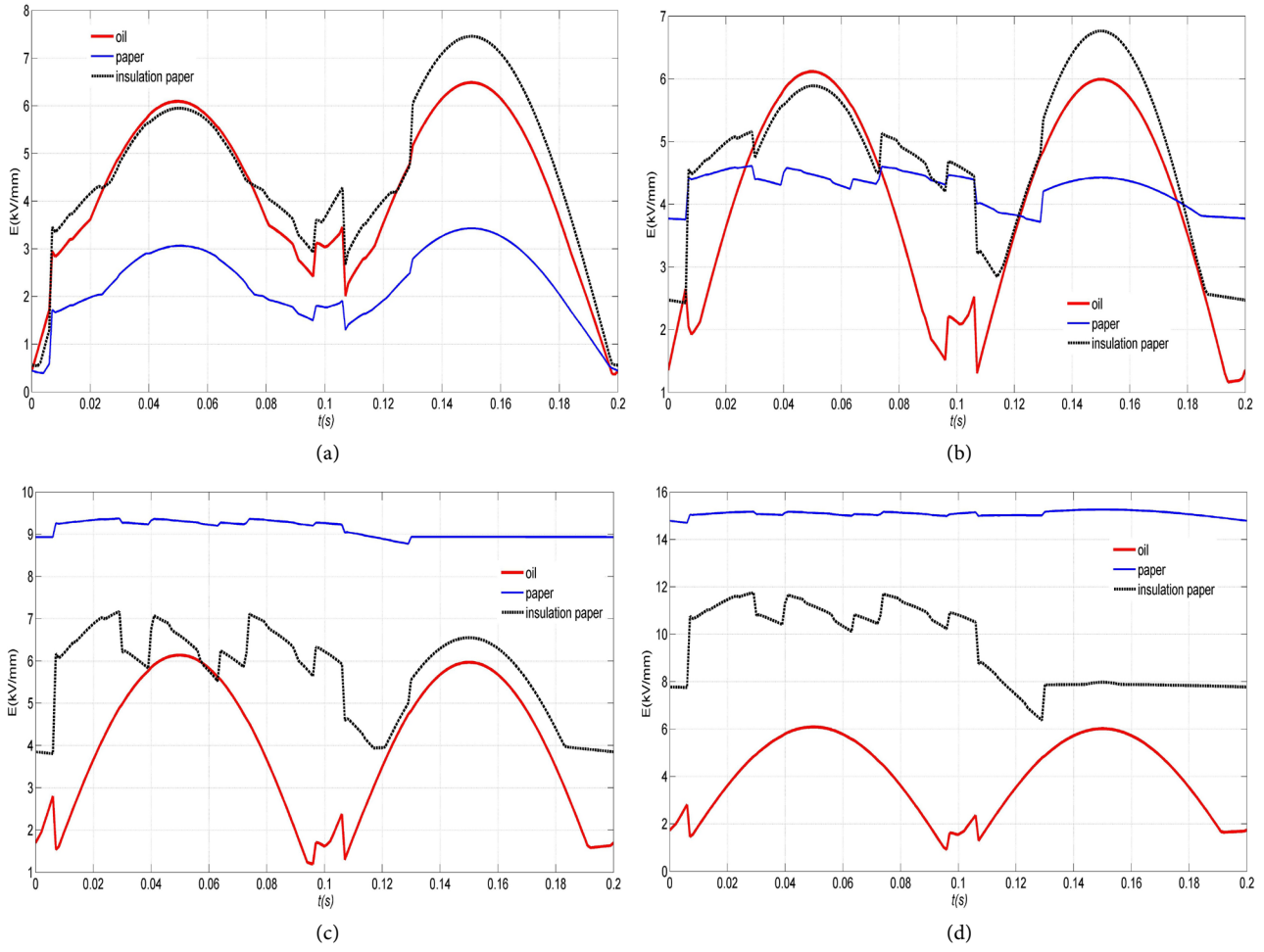

Figure 6. Electric field curves in different materials in a period of the Y_0-Y connected converter transformer. (a) values A1. (b) values A2. (c) values A3. (d) values A4.

Table 2. Maximum Electric Fields of Y0-Y Connected Converter Transformer.

Maximum Electric Fields in Linear Materials (Unit: kV/mm)	Y_0-Y Connected Converter Transformer		
	Oil	Insulation Layer	Oil Immersed Pressboard
A1	9.07	11.23	5.19
A2	6.26	12.77	13.01
A3	6.30	17.27	27.73
A4	6.16	31.06	45.38

Table 3. Maximum Electric Fields of Y0-ΔConnected Converter Transformer.

Maximum Electric Fields in Linear Materials (Unit: kV/mm)	Y_0-Δ Connected Converter Transformer		
	Oil	Insulation Layer	Oil Immersed Pressboard
A1	6.49	7.46	3.43
A2	6.12	6.77	4.61
A3	6.14	7.17	9.37
A4	6.09	11.75	15.26

electric field of oil reduces slightly, and both are important to the transformer insulation.

Acknowledgements

This work is sponsored in part by the National Natural Science Foundation of China under Grant 51407075, in part by the Hebei Province Natural Science Foundation under Grant E2015502004, and in part by the Fundamental Research Funds for the Central Universities of China under Grant 2015 MS79.

References

[1] Zhao, W.J. (2004) HVDC Engineering Technology. China Electric Power Press, Beijing, 318-325.

[2] Wang, C.L. and Li, J.H. (2005) Calculation and Analysis of End Electrical Field in Valve Winding Polarity Reverser Test for Converter Transformer. *Transformer*, **42**, 11-14.

[3] Kurita, A., Takahashi, E., Ozawa, J., *et al.* (1983) DC Flashover Voltage Characteristics and Their Calculation Method for Oil-Immersed Insulation Systems in HVDC Transformers. *IEEE Transactions on Power Delivery,* **PWRD-1**, 184-190.

[4] Lv, X.D. and Chen, D.L. (1997) TheStudy on Electric Field Characteristics of Converter Transformer under Polarity Reversal. *High Voltage Engineering,* **23**, 67-72.

[5] Zhang, Y.L. and Xie, D.X. (2001) Analysis of Transient Electric Field in Converter Transformer. *Journal of Shenyang University of Technology*, **23**, 467-470.

[6] Li, J., Luo, L.F., Xu, J.Z., *et al.* (2016) Study on Electric Charateristics at Ends of Valve Side Winding in Converter Transformer. *High Voltage Engineerin*g, **32**, 121-214.

[7] Chen, Q.G., Zhang, J., Gao, Y., *et al.* (2008) Analysis of Complex Electric Field on Valve Side Widing of Converter transformer. *High Voltage Engineering*, **34**, 484-488.

[8] Ding, Z.G., Li, G.F., Li, P., *et al.* (2008) Electric Field Characteristic Calculation on Typical Oil-Paper Combination Insulation under Polarity Reversal. *Power System Technology*, **32**, 82-85, 90.

[9] Zhang, X.L., Wang, J.M., Wu, Z.B, *et al.*(2009) Numerical Analysis of Electric Field in Valve Side Lead-out Wire for UHV DC Converter Transformer. *Transformer*, **46**, 1-4, 10.

[10] Liu, P., Peng, Z.R., Dang, Z.P., *et al.* (2009) Study on Electric Field Distribution of ±800kV Converting Transformer Bushing Outlet Terminal during Polarity Reversal Test. *Insulators and Surge Arresters*, **3**, 1-4, 8.

[11] Fu, T.J., Wang, J., Zhong, J.T., *et al.* (2009) Insulation Structure Analysis of ±800kV Converter Transformer for DC Transmission. *Transformer*, **46**, 1-5.

[12] Zhang, Y.B., Zheng, J., Wang, D.H., *et al.* (2010) Development of UHVDC Converter Transformer. *High Voltage Engineering*, **36**, 255-264.

[13] Liu, G., Li, L., Li, W.P., *et al.* (2012) Analysis of Nonlinear Electric Field of Converter Transformer under Polarity Reversal Voltage. *High Voltage Engineering*, **38**, 451-456.

[14] Li, Y., Li X.H., Tang, C., *et al.* (2012) Analysis on Transient Electric Field at Ends of Valve-Side Winding in Converter Transformer. *High Voltage Engineerin*g, **38**, 2797-2804.

[15] Li, L., Ji, F., Li, W.P., *et al*. (2011) Numerical Simulation of Converter Transformer's Polarity Reversal Test. *Proceeding of the CSEE*, **31**, 107-112.

[16] Hou, X.M. (2013) The Electric Field Charateristics Simulation of Converter Transformer Valve Side and Analysis of Its Influence Factors. Shenyang University of Technology, Shenyang.

[17] Liu, G., Li, L., Zhao, X.J., *et al*. (2012) Analysis of Nonlinear Electric Field of Oil-Paper Insulation under AC-DC Hybrid Voltage by Fixed Point Method Combined with FEM in Frequency Domain. *Proceeding of the CSEE*, **32**, 154-161.

[18] Zhang, H.F., Liu, G. and Li, H.Q. (2015) Simulation Analysis on Winding Current of Three-Chang ±500kV Converter Transformer under Different Operating Conditions. *Shanxi Electric Power*, **43**, 46-50.

[19] Haus, H.A. and Melcher, J.R. (1992) Electomagnetic Fields and Energy, Translated by Jiang, J.L., Zhou, P.B., Qian, X.Y., *et al*., High Education Press, Beijing, 9-26. (In Chinese)

[20] Yuan, J.S. (1991) Method of Finite Element-Fast Fourier Transformation for Calculation of Linear Time-Dependent Eddy Current Fields. *Journal of North China Institute of Electric Power*, 43-50.